

# IMPACT RESISTANCE OF DIFFERENT TYPES OF LATTICE STRUCTURES MANUFACTURED BY SLM

RADEK VRANA, DANIEL KOUTNY, DAVID PALOUSEK

Brno University of Technology  
Department of Mechanical Engineering  
Brno, Czech Republic

DOI: 10.17973/MMSJ.2016\_12\_2016186

e-mail: [vrana@fme.vutbr.cz](mailto:vrana@fme.vutbr.cz)

The presented paper describes the impact resistance of lattice structure samples made by Selective Laser Melting with the use of AlSi10Mg powder material. The samples with five types of different unit cells of lattice structure were used in this study. The topology of the unit cells structure was changed to describe various impact resistance behavior while the relative density of lattice structure was kept constant. The samples were tested by drop-weight impact testing device with spherical shape of indenter. During the test the maximum reaction force, deceleration and position of load element (indenter) were measured. The results showed, that samples with the same relative density, but with a different shape of unit cell had a different impact resistance. It is because the mechanical properties are significantly influenced by the cell topology which determined the type of failure under loading – bending or buckling. The FBCCZ had the highest impact resistance, but the energy was absorbed with very high reaction force during absorption.

## KEYWORDS

Selective Laser Melting, lattice structure, impact resistance, AlSi10Mg, gyroid, energy absorption, topology

## 1 INTRODUCTION

### 1.1 Selective Laser Melting

Selective Laser Melting (SLM) is an additive manufacturing process for production of metal parts directly from CAD data using a high power laser beam and very fine metal powder with spherical particles. With additive manufacturing process, it is possible to produce components of highly complex shape that cannot be manufactured by conventional technologies. One of the examples is a lattice structure (Fig. 2) which consists of thin trusses or 3D structure [Aremu 2014]. Thus, a lattice structure with good mechanical characteristics and significant reduction of weight can be formed [Yadroitsev 2010].

Lattice structure material produced by SLM is one of many types of light-weight materials which have potential for protective mechanism applications. Currently, the metal foams, honeycomb structures, or balsa wood produced by conventional technologies are used. The advantage of the lattice structure material produced by SLM is that its stiffness can be managed by the geometrical parameters (topology of unit-cell, dimensions of trusses and unit cells, used material) [Yahaya 2015]. Sandwich panels are mostly made up by core and skin. The core is capable of absorbing energy by progressive collapse, while the skins distribute the local vertical load over the impacted area [Labeas 2013].

### 1.2 Mechanical Properties of Different Unit Cells

[Leary 2016] studied mechanical properties of the truss lattice structure made from AlSi12Mg. An experimental study was

performed to find a suitable process parameters for the lattice structure formation and manufacturability testing of different topology of the truss lattice structure. Based on the cube tests (material testing), the optimal parameters of selective laser melting process for AlSi12Mg were found (Laser Power (LP) = 350W; Hatch Space = 0.19 mm; Focal Offset = 2 mm; Laser Speed (LS) = 921mm/s; Layer Thickness = 0.05 mm). Cube porosity of 99.86 % was measured using computed tomography scanning. These parameters were used for manufacture of the tensile specimens for testing of material properties. All results were consistent or exceeded those reported by previous authors or the reported data for die-cast material (Yield strength =  $236.1 \pm 5.4$ MPa; Tensile strength =  $434.1 \pm 14.0$  MPa; Strain to failure =  $4.6 \pm 0.5\%$ ).

The authors identified four possible angles inside the lattice structure unit cell – 0°, 35.3°, 45°, 90°. The angle was 0° qualified as non manufacturable without supporting material. Other angles are self-supported and therefore suitable for lattice structure. The authors also calculated volumetric energy absorption of different types of unit cells and selected prospective candidates. Based on manufacturability of the truss angles, the following unit cells were tested: Body Centered Cubic (BCC), Body Centered Cubic with Z-truss (BCCZ), Face Centered Cubic (FCC), Face Centered Cubic with Z-truss (FCCZ) and Face and Body Centered Cubic with Z-truss (FBCCZ) were tested. The highest compressive strength was found in FCCZ and FBCCZ unit cells.

Production of 3D metal parts using SLM technology allows practically unlimited shape possibilities. However, it applies only to the production using support structures during the production process.

In the case of lattice structures production, it is necessary not to use the support structures. Therefore, the authors [Aremu 2014] investigated mechanical properties for the self-supporting unit cells (BCC, BCCZ, FCC, PFCC, F<sub>2</sub>BCC, gyroid, double-gyroid) via FEM. The results showed that the performance of a lattice structure is largely dependent on the topology of the unit cell.

The authors also found out that the mechanical properties of lattice structure (especially of the truss unit cells) are heavily dependent on the direction of loading. They tested a lattice structure loaded in the x and z directions. Stiffness of the unit cells was significantly lower in the x direction, besides the BCC, gyroid and double-gyroid.

### 1.3 Influence of SLM process parameters on impact resistance

[Shen 2014] studied the lattice structure panels made by SLM from titanium alloy. The results show that the properties of impact resistance of lattice structures are determined by the selective laser process parameters during manufacture. The authors highlighted that the study of properties of lattice-structured material for the use in high-performance lightweight components is required because such results are needed for the FEM analysis of impact.

[Vrana 2016] et al. studied the influence of SLM process parameters on impact resistance of lattice structures. The process parameters were tested directly on small samples of BCC lattice structures (20x20x20 mm, d = 0.6 mm length of unit cell = 4 mm). A tested range of process parameters was as follows: LP = 100 – 400W, LS = 1000 mm/s – 4000 mm/s. The result showed that process parameters significantly influenced the impact resistance of lattice and the dimensions of the trusses of the lattice structure. The graph of maximum transmitted force during impact testing was almost the same character as the graph of increase in truss diameter. The results from [Vrana 2016] confirm the results of [Shen 2014].

The influence of process parameters on the dimensions of single trusses were observed in [Koutny 2014]. The authors manufactured very thin trusses with different orientation (angle) between the truss and the base plate. The authors observed a reduction in the diameter of trusses and sticking of surrounding metal powder at the down skin of the trusses.

#### 1.4 Impact testing

For impact testing, two types of impact testers are mostly used: low-velocity and high-velocity. For high-velocity loading (up to 50 m/s) the horizontal configuration of the tester is mostly used. In this case, a compressed gas pistol is used for initiation of loading [Yahaya 2015]. For low-velocity loading a vertical configuration of impact tester is more suitable. [Shen 2014] and [Mines 2013] examined the ability of various lattice materials with various types of core material to absorb the impact energy. Both of them used the same method for reaction force measurement. They used a deformation element (with a strain gauge) placed between the indenter and falling weight. Mines et al. evaluated the deformation using a laser - Doppler speedometer. Shen et al. used a high-speed camera for measurement of speed and deformation.

In this study, four different types of truss unit cells and one 3D gyroid cell were used for core lattice material inside the sandwich panels. The impact resistance of the samples was tested on the designed drop-weight machine. Results will be used for further development of FEM model and understanding of different types of failure depending on the lattice topology. The samples were made from AlSi10Mg powder which is a very light and common material for SLM application with good mechanical properties.

## 2 MATERIAL AND METHODS

### 2.1 AlSi10Mg Powder Material

AlSi10Mg metal powder from TLS Technik GmbH was used for manufacturing all types of the samples. The powder material with a spherical shape of particles was produced using a gas atomization technology in argon atmosphere. For quality verification, the particle size distribution was analyzed using the particle size analyzer Horiba LA-960. The main parameters of the particle size distribution were as follows – median size 40.7  $\mu\text{m}$ , mean size 41.4  $\mu\text{m}$ , standard deviation 12.9  $\mu\text{m}$ . The particle size up to 25.2 $\mu\text{m}$  represents 10% and particle size up to 58 $\mu\text{m}$  represents 90% of particle size distribution (Fig. 1).

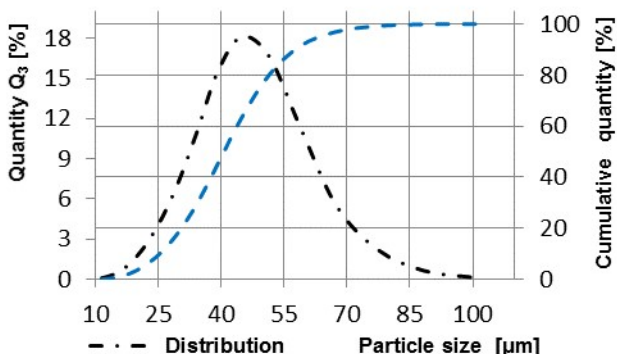


Figure 1. Particle size distribution of the AlSi10Mg metal powder

### 2.2 Selective Laser Melting

The selective laser melting machine SLM 280HL (SLM Solution GmbH) was used for production of all the samples. The machine use one 400W ytterbium laser with Gaussian beam profile for metal powder melting. The size of built volume is

280x280x350 mm. The machine uses a nitrogen or argon atmosphere depending on the used powder material.

The testing samples were manufactured with selected perspective process parameters (Tab. 1) resulting from the previous article [Vrana 2016], where the influence of process parameters and the diameter of the lattice trusses on the impact resistance were investigated.

Position of the samples during building process is shown on the Fig. 3. The samples were manufactured only with support structures on the bottom plate. The lattice structure inside the samples as well as the upper plates were manufactured completely without supports. For the support structures the block type of supports was used.

Table 1. SLM Process parameters

SLM Process Parametres	
Laser speed	1000 mm/s
Power output	350W
Focus offset	1
Layer thickness	50 $\mu\text{m}$
Hatch distance	170 $\mu\text{m}$
Platform heating	120 $^{\circ}\text{C}$
Oxygen level	0.1 – 0.2%
Atmosphere	nitrogen

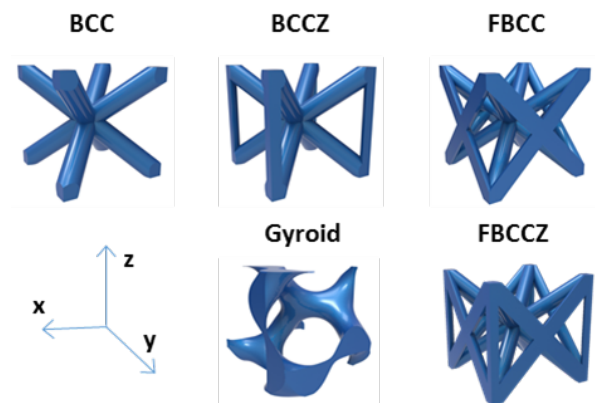


Figure 2. Various types of lattice structure unit cells

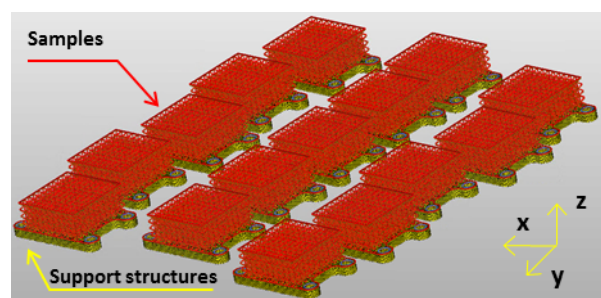


Figure 3. Position of the samples during building process (yellow – Support structures; Red – Samples)

### 2.3 Samples

For mechanical testing, sandwich panels with various types of core material were designed. The samples were composed of top and bottom plates, between which the core material of lattice structure was placed. All parts of the sample were made from AlSi10Mg powder material. In this study, the core material is composed of four types of the truss unit cells (BCC, BCCZ, FBCC, FBCCZ) and one 3D Gyroid (minimal surface) unit cell (Fig. 2). All types were designed with the same level of the relative density 17.9 %. The value of relative density was chosen according to the minimal manufacturable truss diameter from [Koutny 2014] and also according to the results of [Vrana

2015a, Vrana 2015b] where a good stiffness of the core part and the energy absorption without bounce up of the loading element were evaluated. To reach the same value of relative density for all samples with different core material, the diameter in the truss unite cells and parameter  $t$  in gyroid unit cell were changed (Tab.2).

BCC is one of the most common types of unit cell in lattice structures. The cell is composed of eight cylindrical trusses, which corresponds to the space diagonals of the cube. The trusses were inclined by  $35.3^\circ$  relatively to the x-y plane. In this case of BCC lattice structure, the trusses are connected in the center of the cube and at each corner. Under loading the bending type of failure is mainly applied.

BCCZ is a truss unit cell which is composed of twelve trusses. Eight trusses are the same as in the BCC unit cell (space diagonal of the cube). Four more trusses, which connected two corners above (Z direction,  $90^\circ$  to the x-y plate), were added to increase the stiffness of the structure. Under loading, the bending and buckling types of failure are mainly applied.

A FBCC unit cell is composed of twenty-four trusses. Eight trusses (with angle of  $35.3^\circ$ ) were also the same as in BCC. Sixteen more trusses which correspond to the face diagonal (angle of  $45^\circ$  inclined to the x-y plate) of the cube, were added. Under loading, the bending type of failure is mainly applied. The trusses with angle of  $45^\circ$  are more resistant under loading than those with angle of  $35.3^\circ$ .

A FBCCZ unit cell was composed of 28 trusses and combined BCCZ and FBCC unit cells. FBCCZ had trusses with the angle inclined by  $35.3^\circ$ ,  $45^\circ$ ,  $90^\circ$  to the x-y plate. This cell had the highest stiffness of all the cells because the orientation of the trusses enabled the combined bending and buckling loading in common.

One more 3D unit cell was designed, a Gyroid unit cell is a self-supporting minimal surface structure proposed by [Shoen 1970]. For the Cartesian coordinate space  $x, y, z$ , the gyroid surface conforms to the equation:

$$\sin(x)\cos(y) + \sin(y)\cos(z) + \sin(z)\cos(x) - t = 0 \quad (1)$$

where  $t$  is a constant parameter between 0 – 1.413. In this study the parameter was  $t = 0.957$ .

Table 2. Geometrical parameters of the unit cells

Unit Cell	BCC	BCCZ	FBCC	FBCCZ	Gyroid
d (mm)	0.8	0.75	0.6	0.577	-
a (mm)	4	4	4	4	-
t (-)	-	-	-	-	0.957
Trusses	8	12	24	28	-

The samples for impact resistance testing were sandwich panels from AlSi10Mg powder material. The dimensions of the lattice core were  $40 \times 40 \times 16.8$  mm (Fig. 4). The samples were composed of the top ( $t = 0.3$  mm) and bottom ( $t = 0.5$ mm) plates and the lattice structure core in the middle. For placement of the samples to the correct position during the mechanical testing, four holes for bolts were designed in the bottom plate.

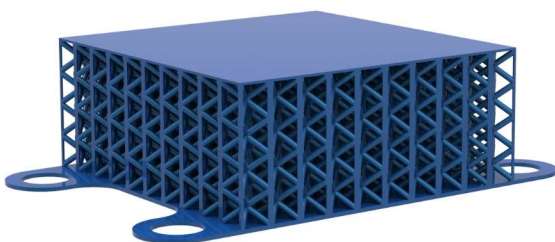


Figure 4. Impact resistance sample with BCC-Z lattice structure

Both plates were machined to ensure straightness for placing and measuring of the sample, using 3D optical scan. Three samples for each type of lattice structure topology were tested ( $3 \times 5$  types).

#### 2.4 Testing of Mechanical Properties

Mechanical properties of all samples were tested using a drop-weight impact tester designed by author (Fig.5). The principle of impact tester is based on a change of kinetic energy of falling head into the impact energy.

The impact tester is equipped with strain gauge XY31-3/120 placed on the deformation element, accelerometer B&K Type 8309 on the top plate of falling head and a high speed camera Phantom V710 in front of the impact tester. Two main sensors (strain gauge and high speed camera) measured the reaction force during penetration of the indenter to the sample and simultaneously also the position of the marker on the falling head. Deceleration measurement using the accelerometer is used only for validation of the designed strain gauge values. Signals from the strain gauge and accelerometer were recorded using the data acquisition system QuantumX MX410B (HBM GmbH) with sampling frequency of 96kHz. The data from the high speed camera were recorded in the Phantom software with sampling frequency of 56 808 Hz. Measured values from all three sensors were evaluated in Matlab software developed for the impact tester. During impact testing the indenter (penetration body) had a spherical shape with diameter  $d = 16$  mm, weight of the falling head was  $m = 2.83$  kg and the drop height was  $h = 1$  m.

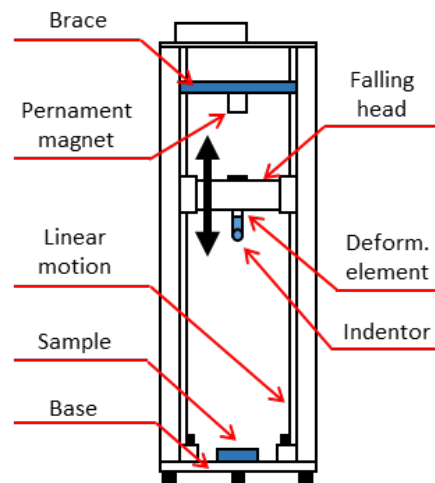


Figure 5. Impact tester

## 2.5 Software data evaluation

Software for data evaluation was compiled in Matlab and is designed for two types of impact measurements, with a high speed camera and a strain gauge and with a strain gauge only. When the high speed camera is used, the software works with measured reaction force from the strain gauge and the position of falling head is obtained from the high-speed camera using the image analysis in Matlab (Fig.6). Software searches the circular mark in the pictures and analyses the coordinates of the circle center in a pixel value.

Due to a different sampling frequency of both sensors the software must recalculate the data record from camera to the frequency of 96 kHz and then it connects these data with the strain gauge in the Force – Position and Position – Time graphs. The software output are two excel files:

- 1) Evaluation of the required parameters such as - penetration (mm), duration of impact (ms), maximal and average force (N), kinetic energy of the falling head (J) - just before impact, rate of the falling head (m/s) - just before impact
- 2) Force – Position, Force – Time, Deceleration – Time, Rate - Time and Position – Time graphs of the single samples and two common graphs for all the samples (Force – Position and Position – Time)

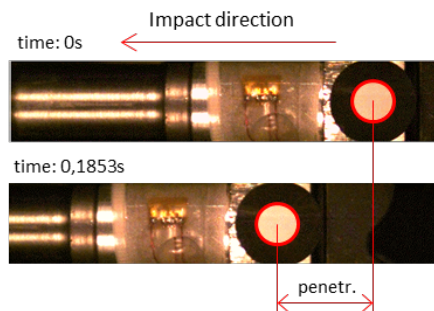


Figure 6. Image analysis in the Matlab software

Otherwise, the position of the falling head is obtained from double integration of deceleration from the strain gauge (deceleration is calculated as a ratio  $a = F / m$ ;  $F$  – reaction force;  $m$  – weight of falling head). A disadvantage of this method is a lower accuracy of evaluation of the penetration. A linear motion also causes significant losses by friction which were not evaluated. This type of measuring is suitable only for comparison of the samples without search for the exact values. Deceleration measuring is evaluated in both cases but it is only used for validation of the strain gauge. In this article, measuring with high speed camera was used.

## 2.6 3D optical measurement

For checking the software evaluation, the depth of deformation (penetration) was measured using 3D optical scanner Atos Triple III Scan (MV170 lens; calibration was carried out according to VDI/VDE 2634, Part 3) and GOM Inspect software. Before the scanning process, the samples were matted with a thin layer of titan powder (around 0,003mm). Penetration was determined using an ideal shape element in the following steps:

- The fitting plane on the upper desk was created (Fig. 7b)
- The imprint of the indenter was used for fitting of the sphere (Fig. 7b)
- The center of the sphere was used to create a perpendicular line to the fitting plane
- Using a perpendicular line, the intersection points were created at the bottom of the sphere and on the fitting plane

- The distance between two previous points were measured as penetration (Fig. 7c)

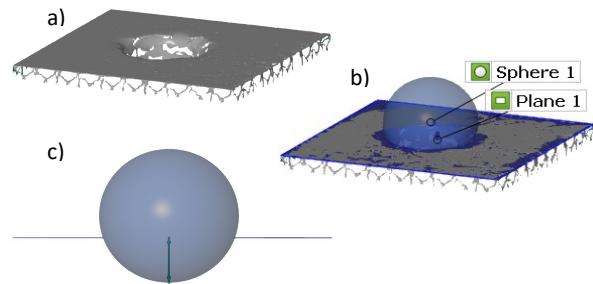


Figure 7 Deviation between different types of the measurement

## 3 RESULTS AND DISCUSSION

The parameters of the produced samples are shown in Table 3. Due to the same relative density of all the samples, the weight should be of the same level. Differences in the weight were mainly caused by sticking of the powder at the down skin of the lattice structure trusses with the angle under 45° (Fig. 8). Because the samples had a different geometry of the structure (number of trusses with angle of less than 45°, a diameter of the truss), the weight of samples was different due to sticking powder. Comparable results were found in [Koutny 2014, Leary 2016].

For checking the software evaluation, penetration was measured using a 3D optical scanner. The results showed (Tab. 4), that the deviation between mechanical testing and 3D optical measuring is up 5% (maximum value was 4,34 %). The real deviation is even smaller because during the impact testing the camera measures both the plastic and elastic deformation of the samples. Using a 3D scanner, only the plastic part of deformation is measured. Table 4 also shows, that *Rate Before Impact* measured with high speed camera is quite constant. It was measured, that *Rate before Impact* has for the same weight of falling head a very small deviation of 0.013 m/s and it can be used to refine of the measurements with strain gauge only.

Two measurements were carried out to determine *Rate before Impact* for fully loaded ( $m = 5.87$  kg) and empty ( $m = 1.83$  kg) falling head (Fig. 10). Based on the finding line, *Rate Before Impact* can be estimated. To obtain more accurate values, measuring of *Rate Before Impact* of more values of weight of falling head must be carried out.

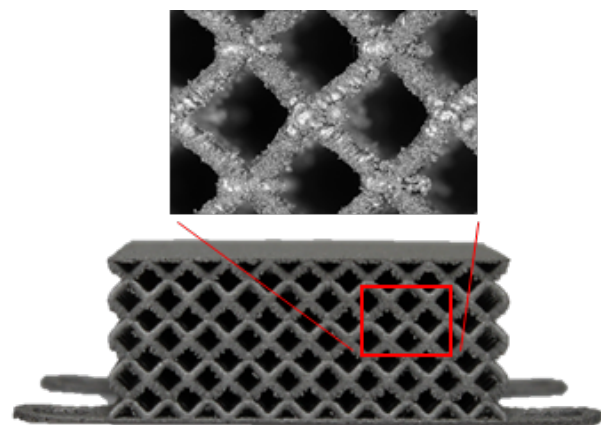


Figure 8. Sticking powder at the down skin of the trusses

Table 3. Parameters of the Samples

Name	CAD Volume (mm <sup>3</sup> )	CAD Surface (mm <sup>2</sup> )	CAD Weight (g)	Real Weight (g)	Avg. Weight (g)	Weight Increase (g)	Weight Increase (%)	Sample Height (mm)	Avg. Sample Height (mm)
BCC1	5978	27398	15.84	15.349	15.97	0.1	1%	16.68	16.76
BCC2				16.265				16.8	
BCC3				16.302				16.81	
BCCZ1	5976	29015	15.84	15.995	15.85	0.01	8%	16.73	16.72
BCCZ2				15.158				16.72	
BCCZ3				16.384				16.72	
FCC1	5999	34866	15.90	20.049	19.87	4.03	25%	16.82	16.80
FCC2				19.685				16.82	
FCC3				19.863				16.77	
PFCC1	5993	36162	15.88	19.399	19.05	3.17	20%	16.75	16.77
PFCC2				18.157				16.76	
PFCC3				19.601				16.8	
SG1	5978	22800	15.84	16.316	15.98	0.14	1%	16.79	16.76
SG2				15.998				16.78	
SG3				15.615				16.71	

As example, the measurement of the BCC2 sample is shown in the picture (Fig. 11) This measurement with camera and strain gauge is considered as a reference. For refining of the penetration when only the strain gauge was used for measurement, the calculated Rate Before Impact ( $v = 4,0139$  mm/s) and theoretical Rate Before Impact ( $v = 4,429$  mm/s) were used. To evaluate the maximum transmitted force only the first peak of the measurement was used. The residual energy was measured as the rate after impact using a high speed camera. Using this value, a kinetic energy after impact and the absorbed energy were finally calculated. All the types of the samples absorbed more than 95% of the impact energy.

The results of measured maximum force showed that the force is not constant for all the samples (Fig. 9).

From the results, it can be seen, that the best impact resistance was achieved by FBCC and FBCCZ structures, because the transmitted high level of the force and the penetration were low. However, if the structure has a high level of impact resistance the ability to absorb is very low. Figure 9 also shows the result of the penetration. For high impact resistance, the low depth of penetration is required.

The result of the impact resistance of different topology of lattice structure could be influenced by sticking of the metal powder at the truss down skin. Table 3 show, that weight of FBCC and FBCCZ was increased by about 20 % and 25 % respectively. For good energy absorption, a long impact and large penetration during the impact loading is necessary.

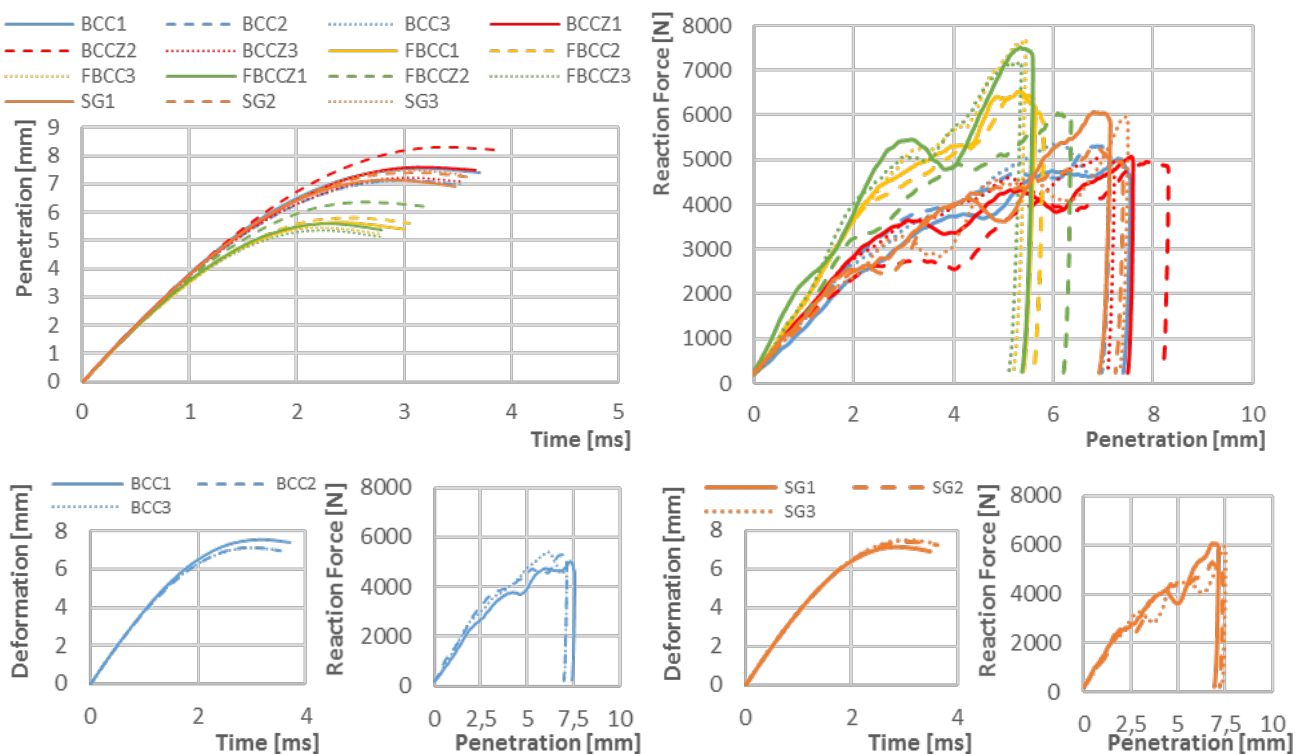


Figure 9 Deviation between different types of the measurement

Table 4. Evaluation of Impact test

Name	Weight of Falling Head (kg)	Penetration Scan (mm)	Penetration Matlab (mm)	Penetration deviation (%)	Rate before Impact (m/s)	Stand. deviation of Impact rate (m/s)	Absorbed Energy (J)	Duration of deformation (ms)	Average Force during test (N)	Maximal Force (N)	Absorption Power (J/s)
BCC1	2,83	-	7,544	-	4,15	0,0130	23,99	3,20	2746	5029	7,50
BCC2		-	7,129	-	4,13		23,60	2,98	2906	5306	7,92
BCC3		-	7,113	-	4,12		23,55	3,00	2871	5381	7,85
BCCZ1		-	7,598	-	4,11		23,56	3,11	2762	5068	7,57
BCCZ2		-	8,306	-	4,13		23,74	3,36	2657	4965	7,06
BCCZ3		-	7,219	-	4,14		23,88	3,06	2840	5108	7,80
FCC1		5,519	5,641	2,21	4,12		23,29	2,39	3337	6526	9,76
FCC2		5,661	5,804	2,52	4,12		23,43	2,52	3285	6431	9,29
FCC3		5,226	5,453	4,34	4,11		23,04	2,22	3579	7672	10,38
PFCC1		5,359	5,590	4,31	4,12		23,24	2,30	3556	7511	10,09
PFCC2		6,208	6,355	2,37	4,10		23,21	2,64	3144	6035	8,81
PFCC3		5,192	5,361	3,25	4,11		23,17	2,22	3517	7185	10,44
SG1		6,929	7,142	3,07	4,13		23,60	2,81	2977	6064	8,39
SG2		7,303	7,396	1,28	4,13		23,69	3,10	2827	5322	7,63
SG3		7,225	7,492	3,70	4,11		23,39	3,07	2869	5966	7,61

Figure 11 Comparison of different evaluation methods

For comparison of lattice structures from this view, the parameter of Absorption Power  $P_a$  [J/s] was defined:

$$P_a = \frac{E_a}{t_a} \quad (2)$$

where  $E_a$  is absorbed energy (J) and  $t_a$  is duration of deformation (s). Absorption power is a characteristic which defined the process of energy absorption during deformation of the sample. If the lattice structure is too stiff, the depth of penetration is very low and the duration of deformation is very short. For slow energy absorption, lower numbers of the Absorption power are suitable.

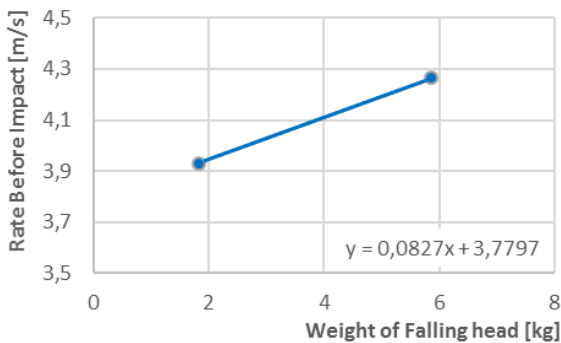
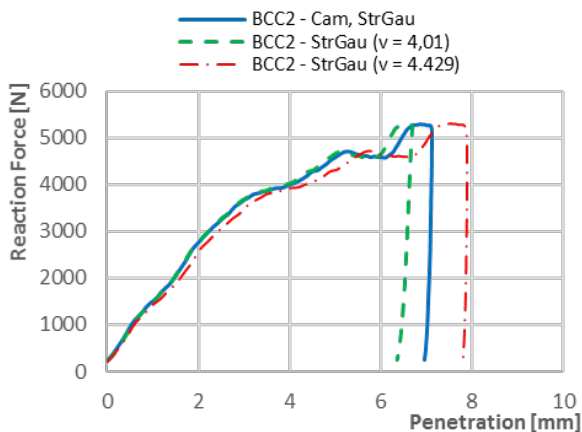


Figure 10 Different values of Rate before Impact depending on the weight



No supports structures were used during the manufacturing of upper plates of the samples. Therefore, the upper plates were manufactured with higher material porosity. It can be seen on the Figure 12. This situation was the same for all the samples and therefore the results from all types of lattice structures can be compared.

#### 4 CONCLUSIONS

- The gyroid structure have similar result as the BCC and BCCZ structure under impact loading. The advantage of the Gyroid is that its stiffness is same for all loading directions.
- For continuous absorption of the energy, long impact and depth of penetration are very important during impact loading. If the time of impact is very short and depth of penetration is low, then the energy is only partly absorbed. For this purpose, the Power of Absorption parameter was defined.
- Friction in the linear motion significantly influenced the impact test. Therefore, for measuring of exact values, the high speed camera must be used.
- Calculated depth of penetration was evaluated with 3D optical scanner. This confirms the correct evaluation in Matlab software.
- Sticking of the powder at the down skin of the trusses could influence the amount of absorbed energy. This is a general problem that occurs during production of lattice structures which needs to be solved in the future.

#### ACKNOWLEDGEMENTS

This work is an output of research and scientific activities of NETME Centre, regional R&D centre built with the financial support from the Operational Programme Research and Development for Innovations within the project NETME Centre (New Technologies for Mechanical Engineering), Reg. No. CZ.1.05/2.1.00/01.0002 and, in the follow-up sustainability stage, supported through NETME CENTRE PLUS (LO1202) by financial means from the Ministry of Education, Youth and Sports under the „National Sustainability Programme I“.

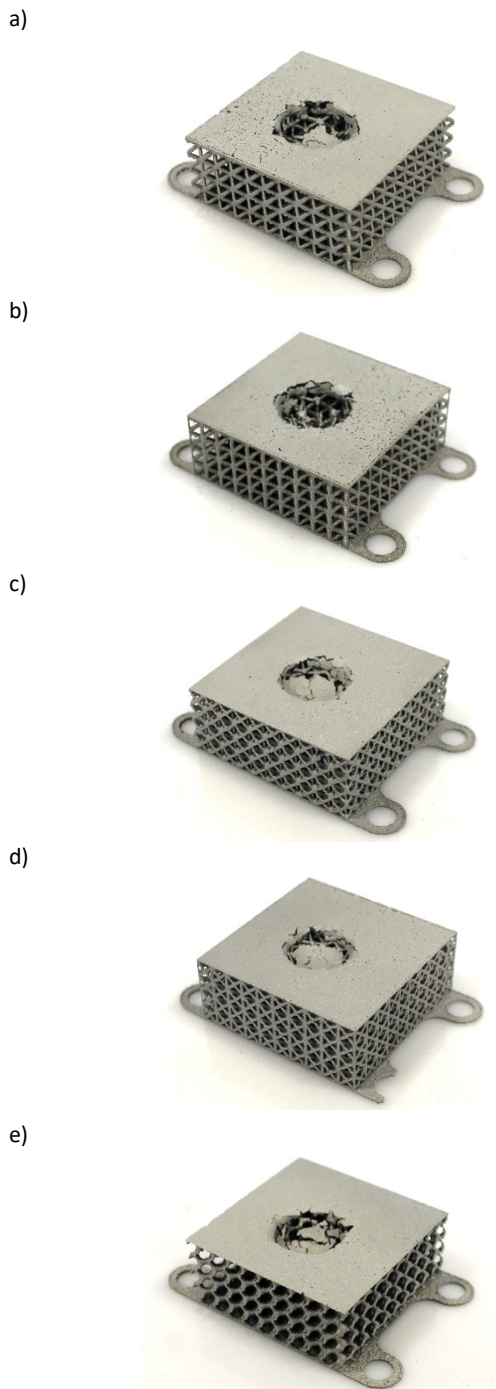


Figure 12. The Samples after impact (a) BCC; (b) BCCZ; (c) FBCC; (d) FBCCZ; (e) Gyroid

## REFERENCES

- [Koutny 2014] Koutny, D. et al. Dimensional Accuracy of Single Beams of AlSi10Mg Alloy and 316L Stainless Steel Manufactured by SLM. 2014. ISBN: 978-961-281-579-0
- [Labeas 2013] Labeas, G. et al. Investigation of sandwich structures with innovative cellular metallic cores under low velocity impact loading. *Plastics, Rubber and Composites* [online]. 2013, vol.42(5), pp 194-202. ISSN 14658011
- [Leary 2016] Leary, M. et al. Selective laser melting (SLM) of AlSi12Mg lattice structures. *Materials & Design* [online]. 2016, vol.98, pp 344-357. ISSN 02641275
- [Mines 2013] Mines, R. A. W. et al. Drop weight impact behaviour of sandwich panels with metallic micro lattice cores. *International Journal of Impact Engineering* [online]. 2013, vol. 60, pp 120-132. ISSN 0734743x
- [Shen 2014] Shen, Y. et al. Low-velocity impact performance of lattice structure core based sandwich panels. *Journal of Composite Materials* [online]. 2014, vol.48(25), pp 3153-3167. ISSN 00219983
- [Schoen 1970] Schoen, A., H. Infinite periodic minimal surfaces without self-intersections, NASA Technical Note D-5541, 1970.
- [Vrana 2015a] Vrana, R. et al. Impact Resistance of Lattice Structure Made by Selective Laser Melting from AlSi12 Alloy. *MM Science Journal* [online]. 2015, vol. 2015(04), pp 852-855. ISSN 18031269. DOI:10.17973/MMSJ.2015\_12\_201547. Available from: <http://www.mmscience.eu/december-2015.html#201547>
- [Vrana 2015b] Vrana, R. et al. Impact resistance of lattice structure made by Selective Laser Melting technology. In *Euro PM2015 Proceedings*. Reims, France: 2015. s. 1-6. ISBN: 978-1-899072-47-7
- [Vrana 2016] Vrana, R. et al. Influence of Selective Laser Melting Process Parameters on Impact Resistance of Lattice Structure made from AlSi10Mg. In *Euro PM2016 Proceedings*. Hamburg, Germany: 2016. s. 1-6.
- [Yadroitsev 2010] Yadroitsev, I. et al. Selective laser melting technology: From the single laser melted track stability to 3D parts of complex shape. *Physics Procedia* [online]. 2010, vol.5, pp 551-560. ISSN 18753892.
- [Yahaya 2015] Yahaya, M. A. et al. Response of aluminium honeycomb sandwich panels subjected to foam projectile impact – An experimental study. *International Journal of Impact Engineering* [online]. 2015, vol.75, pp 100-109. ISSN 0734743x.

## CONTACTS:

Ing. Radek Vrana  
 Brno University of technology  
 Faculty of Mechanical Engineering  
 Department of Mechanical Engineering  
 Technická 2896/2, 616 69 Brno, Czech Republic  
 e-mail: [vrana@fme.vutbr.cz](mailto:vrana@fme.vutbr.cz)  
<http://www.uk.fme.vutbr.cz/>